



Size-resolved atmospheric particulate polysaccharides in the high summer Arctic

C. Leck¹, Q. Gao^{1,*}, F. Mashayekhy Rad^{1,2}, and U. Nilsson²

¹Department of Meteorology, Stockholm University, 106 91 Stockholm, Sweden

²Department of Analytical Chemistry, Stockholm University, 106 91 Stockholm, Sweden

*present address: Department of Chemistry, Umeå University, 901 87 Umeå, Sweden

Correspondence to: C. Leck (lina@misu.su.se)

Received: 20 March 2013 – Published in Atmos. Chem. Phys. Discuss.: 15 April 2013

Revised: 21 November 2013 – Accepted: 25 November 2013 – Published: 23 December 2013

Abstract. Size-resolved aerosol samples for subsequent quantitative determination of polymer sugars (polysaccharides) after hydrolysis to their subunit monomers (monosaccharides) were collected in surface air over the central Arctic Ocean during the biologically most active summer period. The analysis was carried out by novel use of liquid chromatography coupled with highly selective and sensitive tandem mass spectrometry. Polysaccharides were detected in particle sizes ranging from 0.035 to 10 μm in diameter with distinct features of heteropolysaccharides, enriched in xylose, glucose + mannose as well as a substantial fraction of deoxysugars. Polysaccharides, containing deoxy-sugar monomers, showed a bimodal size structure with about 70 % of their mass found in the Aitken mode over the pack ice area. Pentose (xylose) and hexose (glucose + mannose) had a weaker bimodal character and were largely found with super-micrometer sizes and in addition with a minor sub-micrometer fraction. The concentration of total hydrolysable neutral sugars (THNS) in the samples collected varied over two orders of magnitude (1 to 160 pmol m^{-3}) in the super-micrometer size fraction and to a somewhat lesser extent in sub-micrometer particles (4 to 140 pmol m^{-3}). Lowest THNS concentrations were observed in air masses that had spent more than five days over the pack ice. Within the pack ice area, about 53 % of the mass of hydrolyzed polysaccharides was detected in sub-micrometer particles. The relative abundance of sub-micrometer hydrolyzed polysaccharides could be related to the length of time that the air mass spent over pack ice, with the highest fraction (> 90 %) observed for > 7 days of advection. The aerosol samples collected onboard ship showed similar monosaccharide com-

position, compared to particles generated experimentally in situ at the expedition's open lead site. This supports the existence of a primary particle source of polysaccharide containing polymer gels from open leads by bubble bursting at the air–sea interface. We speculate that the occurrence of atmospheric surface-active polymer gels with their hydrophilic and hydrophobic segments, promoting cloud droplet activation, could play a potential role as cloud condensation nuclei in the pristine high Arctic.

1 Introduction

The ability to explain the occurrence of the high Arctic cloud condensation nuclei (CCN) is a critical element in improving our ability to assess the potential role of Arctic low-level clouds on the melting and freezing of the perennial sea ice (Intrieri et al., 2002; Sedlar et al., 2011; Tjernström, 2005). For the first time, recent unique results have confirmed that polymer gels in atmospheric aerosols and in clouds originate from seawater (Orellana et al., 2011). These results strongly support the previously unverified hypothesis of a link between cloud formation and polymer gels in the surface microlayer (SML, < 1000 μm thick at the air–sea interface) of the high Arctic open leads (Bigg et al., 2004; Leck and Bigg, 1999, 2005b, 2010; Leck et al., 2002; Bigg and Leck, 2008). The high Arctic open leads can be described as ever-changing open-water channels comprising 10–30 % of the ice pack ice area, ranging from a few meters up to a few kilometers in width.

Polymer gels, also referred to as marine gels, are produced by phytoplankton and sea ice algae biological secretions. These polymer molecules are non-water-soluble, highly surface-active and highly hydrated (99 % water) polymer saccharide molecules. They combine spontaneously to form three-dimensional networks, inter-bridged with divalent ions ($\text{Ca}^{2+}/\text{Mg}^{2+}$), to which other organic compounds, such as proteins and lipids, are readily bound (Decho, 1990; Chin et al., 1998; Zhou et al., 1998; Verdugo, 2012; Xin et al., 2013). The marine gels span the whole size spectrum from 2–10 nm in diameter (colloidal nanogels containing single macromolecules) up to micrometers (colloidal microgels can aggregate to several hundred micrometers). Moreover, the Arctic gels have also been shown to consist of hydrophilic and hydrophobic segments (Orellana et al., 2011) in agreement with their chemical behavior modeled by Xin et al. (2013). The interaction of the hydrophilic and hydrophobic entities on the behavior of the three-dimensional polysaccharide structures during the cloud droplet activation strongly suggests a dichotomous behavior for polymer gels (Ovadnevaite et al., 2011); an only partial wetting character is seen below 100 % relative humidity (RH), thus showing only weak hygroscopic growth, but at the same time a high CCN activation efficiency is shown, which is promoted by the hydrophilicity or surface-active properties of the gels.

Blanchard (1971) and Blanchard and Syzdek (1988) have long advocated that a significant fraction of the remote oceanic aerosol is derived from two distinct processes when bubbles on seawater burst. One is from fragments of the bubble membrane (film) that are injected into the air when the bubble bursts (“film drops”: centered on about 100 nm diameter). The other is from drops of water that are detached from an upward-moving jet of water that follows the bubble burst (“jet drops”: centered around 1 μm diameter). Breaking waves, induced by wind stress at the air–water interface, are known to be a major source of bubbles in the open ocean, entraining air into the ocean surface layer. Over the Arctic pack ice, however, near-surface winds are generally weak ($<6 \text{ m s}^{-1}$ 70 % of the time; Tjernström et al., 2012) and the open-water fetch is small in the open leads. In the pack ice region, whitecaps do occur in sufficiently high winds of ca. 15 m s^{-1} , but the waves are very small compared to those over the open ocean. As a result breaking waves are in general rare or absent, and it has therefore been unclear whether bubbles exist in the absence of white capping in the central Arctic Ocean environment (Leck et al., 2002). Even in the absence of wind-driven breaking waves a recent study has now confirmed both the presence and temporal variability of a population of bubbles within the open leads (Norris et al., 2011). The bubble concentrations are comparable with those observed in the open ocean under modest wind speeds (order of 10 m s^{-1}), but decrease more rapidly with increasing bubble size. A non-wave bubble source mechanism, subsequently generating both film and jet drops, driven by the surface heat flux was proposed. The open leads are

low-turbulence environments, so the upper surface layer can reach equilibrium for dissolved gases – if cooled (heat flux to atmosphere) the solubility of gases will increase above that of the bulk water. Eventually cooling is sufficient to allow surface water to sink convectively. Mixing with warmer water then decreases solubility and forces dissolved gases out of solution to form bubbles. As the bubbles rise through the water prior to their injection into the atmosphere, they have been documented to scavenge sea salt, fragments of phytoplankton, bacteria, viruses and high-molecular-weight soluble organic surface-active compounds (Blanchard and Woodcock, 1957; Blanchard, 1971; Blanchard and Syzdek, 1988; Gershey, 1983; O’Dowd et al., 1999). However, studies of individual particles by Bigg and Leck (2001, 2008), Leck et al. (2002), and Leck and Bigg (2005a, b) over the perennial ice have failed to find evidence of sea salt particles of less than 200 nm in diameter. To explain this, the same authors proposed a bubble-induced mechanism responsible for transporting polymer gel-rich organic material from the bulk seawater into the open lead SML. It was suggested that the highly surface-active polymer gels could attach readily to the surface of rising bubbles and self-collide to form larger aggregates. Consequently, polymer gels and their aggregate production, as well as the embedded solid particles such as bacteria, phytoplankton and its detritus, can be carried selectively to the surface microlayer by rising bubbles. Before bursting, bubbles stay in the microlayer for some time and therefore are likely to acquire walls, consisting to a large extent of strengthening gels, with embedded particulate matter that may be points of weakness as the water drains from between the walls. Following the burst, the film drop fragments would not be drops of salt water but of gel material with salt-free water and any particles attached to the fragments. Even though jet drop particles are mainly composed of sea salt, over the Arctic pack ice area they have been observed to be partly coated by polymer gels (Leck et al., 2002).

The presence of the polymeric gels of open lead origin in the high Arctic atmospheric aerosol and cloud droplets was recently demonstrated (Orellana et al., 2011). The authors used a novel immunological technology and highly specific antibody for seawater biopolymers. The combined value of using electron microscopy for detection of single particles composed of polymer gel material, bacteria in the absence of sea salt, as well as sea salt particles associated with the same gel material has been clearly shown for atmospheric samples collected both in the pristine high Arctic summer and at remote marine locations at lower latitudes (Bigg, 1980, 2007; Gras and Ayers, 1983; Posfai et al., 2003; Leck and Bigg, 2008). Based on the technique of nuclear magnetic resonance spectra, Fourier transform infrared spectra, X-ray spectromicroscopy and Alcian blue staining (Kuznetsova et al., 2005) a few more studies at lower latitudes have shown that the chemical nature of the organics in marine aerosol particles resembles biogenic organics containing polysaccharides from seawater. The former studies were performed at

Barrow, USA (71° N, 156° W), and in the Arctic Ocean south of the ice (Hawkins and Russel, 2010; Russell et al., 2010), in the North Atlantic Ocean (Facchini et al., 2008), as well as in the eastern South Pacific (Hawkins and Russell, 2010).

Whereas these methods have proven very useful for the understanding of the multi-component and multi-phase nature of ocean-derived aerosol particles, they are not completely quantitative (the immunological technique excluded). Furthermore, obtaining statistics of the proportion of particles having a particular property promoting cloud-nucleating abilities is very time-consuming. Strengthening the quantitative information of the contribution of polymer gels to the marine aerosol necessitates the possibility for detection of mass. This is further challenged in the high Arctic summer due to the very low total atmospheric suspended particulate matter (less than 10 µm in diameter) observed, with median concentrations of 0.9 µg m⁻³ (Leck and Persson, 1996a).

This paper will reveal unique chemical fingerprints of atmospheric size-resolved polymer gels. The ultimate aim is to provide information relevant to the CCN control of albedo of the persistent low-level clouds in the summer Arctic and with influence on the melting and freezing of the perennial sea ice. The samples were collected at the open waters along the ice edge and from within the perennial pack ice of the central Arctic Ocean during the biologically most active period from the late summer melt season and into the transition to autumn freeze-up. A novel analytical method was used utilizing liquid chromatography (LC) coupled with highly selective and sensitive tandem mass spectrometry (MS–MS) with a triple-quadrupole mass spectrometer. However, there can be thousands of different polysaccharide in the phytoplankton and sea ice algae secretions. The building block monomers of the polysaccharides (monosaccharides) can also be joined together in various orders or with different functional groups. Even more, the polysaccharides can be linear or branched. The polysaccharides differ from each other by the degree of polymerization (the number of repeated units of monosaccharides) and will thus differ in their molar masses. This variety in molar mass allows for multiple mass-to-charge (m/z) ratios, which together with low abundances makes their determination by spectrometry extremely difficult. Monitoring a specific m/z ratio leads to a drastic drop in signal intensity. Furthermore, a triple-quadrupole mass spectrometer has an upper m/z limitation. To overcome these analytical obstacles, the combined polysaccharide molecules collected were fragmented by hydrolysis into their monosaccharide units prior to determination. One very significant benefit with this approach is that conclusions can be drawn concerning the origin of the polymer gels (cellular materials, of phytoplankton: *pentoses and hexoses*; or exudates from phytoplankton and/or non-photosynthetic microbial bacteria: *deoxysugars*) (Panagiotopoulos and Sempere, 2005; Skoog and Benner, 1998). The following seven monosaccharides were targeted, as they constitute the backbone of polysaccharides for algae and their exudates: *pentoses*: xylose and arabinose; *hexoses*:

glucose, mannose and galactose; and *deoxysugars*: rhamnose and fucose. The sum of these seven monosaccharides is referred to as total hydrolysable neutral sugars (THNS) in the text to follow.

2 Study area and experimental approach

2.1 Location

Quantitative determination of the seven targeted monosaccharides in atmospheric aerosols was performed as part of the Arctic Summer Cloud and Ocean Study (ASCOS) onboard the Swedish icebreaker *Oden* in 2008. The interdisciplinary program was conducted in the fields of marine biology and chemistry, atmospheric chemistry, oceanography and meteorology with the overall aim to improve our understanding of low-level cloud formation and possible climate feedback processes over the central Arctic Ocean.

The expedition departed from Longyearbyen, Svalbard, on 2 August 2008 (day Of year, DOY, 215), and headed north for the pack ice of the central Arctic Ocean. There was a transition from the “marginal ice zone” having 20–70 % ice cover to the “pack ice region” with 80–95 % ice cover. Measurements commenced on 12 August (DOY 225), when *Oden* was anchored to a large ice floe (referred to as the pack ice drift, or PI-drift), slightly north of 87° N (87.4° N; 1.5° W), and proceeded to drift with the ice floe for the following three weeks, until midnight between 1 and 2 September (DOY 245–246) (87.1° N, 12° W) to return southwards. On the way to the large ice floe additional brief stations were set up: an open-water station (OW1) in the Greenland Sea on 3 August 2008, 00:00 to 12:00 (DOY 216–216.5) (78.2° N; 7.5° E), followed by a 24 h station in the marginal ice zone (MIZ1) starting on 4 August 2008, 12:00 (DOY 217.5) (79.9° N; 6.1° E). On the way back, a second marginal ice edge station (MIZ2) was set up at the ice edge on 6 September 2008, 09:00, to 7 September 2008, 04:00 (DOY 250.4–251.2) (80.7° N; 8.9° E), immediately followed by a final 12 h open-water station (OW2) ending on 7 September 2008, 16:00 (DOY 251.7) (80.4° N; 10.1° E), in the Greenland Sea before arriving at Longyearbyen on 9 September (DOY 253). A map of the route with the ice drift magnified is shown in Fig. 1. All times are reported in Coordinated Universal Time (UTC). The Sun was continuously above the horizon of the expedition. For further cruise details see Paatero et al. (2009) and Tjernström et al. (2013).

2.2 Atmospheric sampling of aerosol particles onboard ship

In order to optimize the distance both from the sea and from the ship's superstructure, the sampling inlet for atmospheric aerosol particles extended at an angle of 45° to about three meters above the container roof on the 4th deck, about 25 m above sea level. An Andersen impactor (Anderson Inc.,

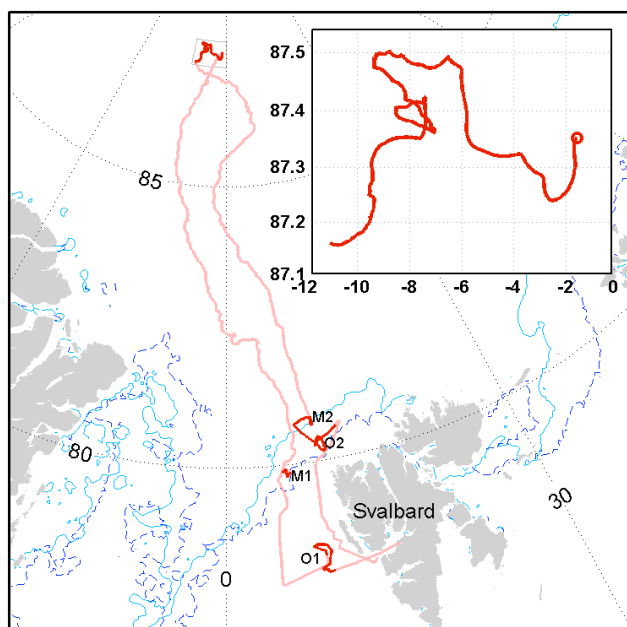


Fig. 1. Map of the ASCOS cruise track (pink) with ice-drift period (PI-drift) highlighted (red) and (inset) shown in detail, with the start of the drift marked by the circle. The left-hand part of the track shows the initial northward track, while the right-hand track shows the southward, return track. Convolute track lines in open water, OW (O1 and O2), and at the ice edge, MIZ (M1 and M2), are associated with shorter sampling stations. The dashed light-blue line illustrates the ice edge at the time of entry and the darker-blue line at the time of exit.

Atlanta, GA, USA) at the top of the sampling line excluded particles $D_p > 10 \mu\text{m}$ (PM_{10}) in equivalent aerodynamic diameter (EAD) at ambient RH. The total flow through the 9 cm inner diameter sampling line pipe was 1140 L min^{-1} , which resulted in a residence time of $< 1.4 \text{ s}$ and a Reynolds number of 21 000. The turbulent flow in the main inlet (no bend) ensured that the particle concentration was homogeneous across the duct due to the mixing caused by the turbulent eddies; hence the sampling inlet can be considered as creating a homogenous particle field in the duct. A disadvantage is that particle losses to the walls of the duct are increased: the extent of the losses is a factor that depends on the flow regime, particle aerodynamic size, and duct surface roughness (von der Weiden et al., 2009). The estimated particle losses were calculated to be less than 0.5 % for particles below 1000 nm in diameter. The corresponding number for the larger particles up to $10 \mu\text{m}$ in diameter was 5 %.

The air was sampled using isokinetic secondary lines connected to the sampling impactors in use. Upstream of the impactors, the temperature and the RH of the incoming sample air were measured and recorded using miniprobes and a data acquisition system custom-made for the expedition by Vaisala. The PM_{10} inlet was identical to the one used during three previous expeditions to the same area and time of year

(Leck et al., 1996, 2001, 2004); details on its position and design on board the *Oden* are further described in Leck et al. (2001).

To maximize the sampling time, i.e., to exclude contamination from the ship and from on ice activities, it was required that the mast was facing upwind. During the PI-drift this necessitated a “harbor” in the ice in which the ship, with its non-rotating mast on the 4th deck, could be moored in several different directions and turned as the wind direction changed. To further ensure uncontaminated sampling, direct contamination from the ship’s exhaust and infrastructure was excluded by using a pollution controller, turning off all the pumps of the sampler, in direct connection to the sampling manifold. It consisted of a TSI-3025 counter connected to the control system described by Ogren and Heintzenberg (1990). The quality of the samples was additionally monitored using various combustion tracers and wind speed – and direction – thresholds: provided that the wind was within $\pm 70^\circ$ of the direction of the bow and stronger than 2 m s^{-1} , no ship pollution reached the sample inlets. Further details of the location and properties of air intakes and instruments, position on the ship, pumping arrangements and precautions to exclude contaminated periods can be found in Leck et al. (2001) and in Tjernström et al. (2013).

Low-pressure Berner cascade impactors (BCIs) (Berner et al., 1979) were used to collect samples for a quantitative determination of the hydrolyzed polysaccharides at 45–50 % RH. The flow rate of sampling was 77 L min^{-1} . In the early stages of the voyage the BCIs collected enough material for analysis in 20 h, but later in the voyage sampling times had to be extended to as long as 40 h. Field blank samples were obtained by setting the impactors with loaded substrates at the sampling site during the same sampling period, but without air passing through. In total, 18 duplicate BCI samples were collected during the course of ASCOS.

The BCIs collected particles in the size ranges < 0.161 (stage 1, back-up), $0.161\text{--}0.665$ (stage 2), $0.665\text{--}2.12$ (stage 3), $2.12\text{--}5.0$ (stage 4), $5.0\text{--}10 \mu\text{m}$ (stage 5) EAD (50 % collection efficiency). Converted to dry (20 % RH) geometric mean diameters, the BCI size ranges corresponded to < 0.113 , $0.113\text{--}0.489$, $0.489\text{--}1.58$, $1.58\text{--}3.73$ and $3.73\text{--}7.47 \mu\text{m}$. In comparison with Covert et al. (1996), the BCIs with five stages thus enabled detection of chemical composition in Aitken mode (lowest stage), accumulation mode (stage 2) and coarse mode (stages 3–5). Millipore Fluoropore membrane filters (pore size $1.0 \mu\text{m}$; diameter 47 mm) were used for stage 1. The Millipore filter has a 99 % collection efficiency for particles with diameters larger than $0.035 \mu\text{m}$ (Liu and Lee, 1976). Pre-cleaned Tedlar[®] polyvinyl fluoride films (DuPont) were used as particle impaction substrates for the other four stages. Ambient samples and blanks were carefully handled in a glove box (free from particles, sulfur dioxide and ammonia) both prior to and after sampling. All substrates for determination of organic compounds were

flash-frozen in liquid nitrogen directly after unloading and stored at -80°C until further treatment.

2.3 In situ generation of nascent aerosol by artificial bubble bursting at an open lead site

The bubbling experiments were made at a field site located at the edge of an open lead approximately 3 km from the *Oden*. The width of the open lead varied from day to day with the movement of the ice from around 20 m to 100 m. From a floating platform approximately two meters from the edge of the ice floe, filtered, particle-free air was released under water through two porous sintered glass frits (nominal pore size 15–25 μm) with their heads located 12 cm below the water surface. Under these conditions, the bubbles burst immediately at the air–sea interface. The bubbling source was driven by a battery-operated pump at a flow rate of 200 mL min^{-1} , which generated a sufficient number of bubbles of about 500 μm in diameter. These artificially generated bubbles are realistic in size but, at the upper end of the observed size distribution, range 30–560 μm (Norris et al., 2011). Two filter holders were placed above the bubble-bursting region at a height of 13 cm above the water surface. The nascent particles were collected onto pre-cleaned nylon filters with 50 % collection efficiency at 1 μm diameter using a vacuum pump with a flow rate of 18 L min^{-1} . Collection times lasted from 30 min to 3 h. With this set-up it was difficult to assess quantitatively how much of the aerosol produced was actually collected. However, the artificial production of bubbles amplified the natural bubble-bursting process dramatically. Therefore, even with collection times of 30 min, an aerosol sample sufficiently large for subsequent analysis was collected. The necessary corresponding sampling time for the atmospheric samples was 40 to 80 times longer. Due to the close proximity of the filter holders to the water surface, and due to the extremely clean conditions during the high Arctic summer, we consider the influence of ambient gases and aerosol on the nascent particles to be minor.

2.4 Determination of hydrolyzed polysaccharides

The aerosol particles including the polymer gels (polysaccharide molecules) collected on the substrates or filters were ultrasonically extracted with ultrapure water (Milli-Q, resistivity 18.2 $\text{M}\Omega\text{ cm}$). The samples were vacuum-dried and then hydrolyzed to monosaccharides with 4 M trifluoroacetic acid (TFA) at 100°C for 2 h. The hydrolysate after removal of excess TFA was reconstituted in acetonitrile and water (80 : 20, v/v). Details about the hydrolysis procedures are given by Gao et al. (2010). Determination of the seven targeted monosaccharides (*pentoses*: xylose and arabinose; *hexoses*: glucose, mannose and galactose; and *deoxysugars*: rhamnose and fucose) was carried out using LC–MS–MS. Chromatographic separation was performed at room temperature using an aminopropyl-silica col-

umn (150 mm \times 2.1 mm, 5 μm , Zorbax NH_2 , Agilent Technologies, Santa Clara, CA, USA), with a mobile phase composed of acetonitrile and water (80 : 20, v/v). The system was operated under isocratic conditions with a flow rate of 400 $\mu\text{L min}^{-1}$. Injection volume was 5 μL . The LC system (Accela, Thermo Fisher Scientific) was coupled to a triple-quadrupole mass spectrometer (TSQ Vantage, Thermo Fisher Scientific, Waltham, MA, USA) equipped with a heated electrospray ionization (ESI) interface operating in negative mode. Quantification was undertaken in selected reaction monitoring (SRM) mode with deprotonated monosaccharides as precursor ions ($[\text{M}-\text{H}]^{-}$, corresponding to m/z ratios 179, 163 and 149) and monitoring fragment ions at m/z 59 and 89. The main MS conditions were as follows: ionization voltage 3.5 kV; capillary temperature 300°C ; vaporizer temperature 250°C ; collision gas pressure (Ar) 0.5 mTorr; and mass resolution 0.7 Da for both the first and third quadrupoles. More information about instrumental working parameters are given by Gao et al. (2011).

The chromatographic peaks from glucose and mannose were not fully resolved. However, their identical response factors made it possible to quantify them together. The sum of the sugars glucose and mannose is referred to as “glucose + mannose” in the following text. The relative standard deviation (%RSD) values, as a measure of precision, was below 12 %, and the instrumental limits of detection (LOD) were in the range 0.7–4.2 pg injected onto the column (Gao et al., 2011). To make sure that our results were not biased by naturally occurring free monosaccharides, samples of SML were compared for all the seven targeted monosaccharides. No free monosaccharides except for glucose could be detected in any of the samples. For glucose the molar ratio of free monosaccharides to hydrolyzed polysaccharides was 2 %.

All determinations were corrected for blank levels and expressed in pmol m^{-3} at standard temperature and pressure (STP; 273.15 K and 1013.25 hPa).

3 Data sets and data processing

3.1 LC–MS–MS determination

Triple-quadrupole LC–MS–MS with ESI in SRM mode, as utilized in this study, is a highly selective technique. The two filtering stages for the specific precursor-to-fragment transitions enabled substantial reduction of the sample matrix interferences, with improved LOD as a result. This is of great advantage for the determination of trace-level monosaccharides within a complex matrix including the interfering substances from collection substrates (e.g., Tedlar film or Teflon filters), the biological matrix (i.e., peptides and lipids associated with gels) and the inorganic sea salts, which could account for a large part of the super-micrometer aerosol mass (Leck and Persson, 1996a; Leck et al., 2002). The method

has been evaluated previously regarding linearity, accuracy, precision, matrix effects and LOD (Gao et al., 2011). For the application to aerosol mass determinations, the accuracy was revalidated by analyzing replicates of blank filter samples spiked with monosaccharide standards at two concentration levels (40 and 200 ng mL⁻¹) and thereafter treated in the same way as the ambient aerosol samples. LOD and limits of quantification (LOQ) of the analytical method (IUPAC, 1978) were defined as 3 and 10 times, respectively, the standard deviation (SD) of the results from the blank filters. LOD were shown to range from 6.4 to 12.6 ng mL⁻¹. By assuming a sampling volume of 100 m³ of air (24 h sampling at the designated BCI flow rate of 77 L min⁻¹), the quantification of monosaccharides (hydrolyzed polysaccharides) in levels as low as 0.13–0.28 pmol m⁻³ would be possible. Duplicate BCI sample including the seven target monosaccharides agreed on average within 25 %. To our knowledge this application of LC–MS–MS to measure naturally occurring polysaccharides in atmospheric aerosols over a remote marine area is novel. The results of method validation are summarized in Table 1.

3.2 Backward trajectories and time spent over the pack ice

The vertical structure of the atmosphere was typical for central Arctic summer during the expedition. The air layer closest to surface was shallow and well mixed with depths usually below 200 m. The atmospheric boundary layer (ABL) was capped by a temperature inversion with a stable stratification of the atmosphere aloft due to the advection of warmer air masses from the south (Tjernström et al., 2012). The NOAA HYSPLIT (Hybrid Single-Particle Lagrangian Integrated Trajectory) model (Draxler and Rolph, 2011; Rolph, 2011) was used to calculate three-dimensional five- and ten-day backward trajectories of the air reaching *Oden's* position. The trajectory calculations were based on data from the Global Data Assimilation System (GDAS) of the National Weather Service's National Center for Environmental Prediction (NCEP). Vertical motion in the trajectory runs was calculated using the model's vertical velocity fields.

The backward trajectories were calculated for an arrival height in the well-mixed layer within the ABL, 100 m above surface level, at hourly intervals. The height of 100 m is a compromise to ensure that at least the receptor point is fairly close to the surface where the samples were collected (25 m above sea level), and at least in the well-mixed layer, but also that trajectories, due to rounding errors and interpolation, would not run too great a risk to “hit the surface” in the backward-trajectory calculations. To use *Oden's* position as a starting point of the backward-trajectory calculations gave a point that is very precisely measured with GPS. Backward trajectories have several sources of uncertainty, which generally grows with the length of the trajectory. Most uncertain is transport in the vicinity of strong gradients, such as

frontal zones, while within a single air mass the trajectory calculations are likely more reliable. For the extent and distribution of the pack ice, ice maps from the satellite sensor AMSR-E, “level 1A” with the data sourced from NSIDC (Boulder), United States, finalized at Bremen University, <http://iup.physik.uni-bremen.de:8084/amr/amre.html> were used.

With the help of the back trajectories and ice maps the time elapsed since the air was last in contact with the open ocean was computed in the way that Nilsson (1996) reported. It will be referred to as days over ice (DOI). The calculated DOI thus marks the end point for an air parcel that left the ice edge 0–10 days ago (resolved by the length of the trajectories). The measure of DOI will in the later analyses (see Sect. 6.2) be used as a simple parameter to summarize the evolution of the aerosol as a function of the synoptic-scale systems since their last contact with open sea. Calculated cumulative travel times over ice for ASCOS showed that most trajectories spent at least three days (median 3.3 days) over the pack ice before reaching *Oden*. Travel times less than two days were encountered around 30 % and travel times of four days and longer covered about 40 % of the cases.

4 Conditions influencing the sources, sinks and transformations of the polymer gels in the atmosphere

The synoptic-scale systems advecting heat, moisture, and particulate matter from the ice edge and open water in between the ice floes, for a variable length of time over the pack ice, will affect the chemical and physical transformations and hence properties of the observed particle size distributions at the location of the ship. Tjernström et al. (2012) summarize the meteorological conditions during ASCOS. From August to early September in 2008, the meteorology was characterized by high pressure over the Canadian Basin and low pressure over northern Norway into the Kara Sea, which generated an anti-cyclonic large-scale flow over much of the central Arctic Ocean. As a result, several low-pressure systems propagated westward, around the North Pole and across the path of ASCOS in the North Atlantic sector of the Arctic, especially during the first half of the expedition (DOY217 to DOY228). After this, the synoptic-scale weather became more inactive (DOY229 to DOY243), with the formation of a high-pressure system over Svalbard, which moved slowly towards and across the North Pole and dominated the weather conditions from DOY244 almost until the end of the expedition. This gave a variety of cloud conditions, including deep frontal systems with heavy snow, complex multi-layered systems, boundary layer fogs, and persistent low-level stratiform mixed-phase clouds. In all, clouds occurred more than 90 % of the time. In general conditions were consistently very moist, with relative humidities rarely under 90 %, while near-surface winds were most often (70 % of the time) in the

Table 1. Accuracy, precision, relative standard deviation (%RSD), limits of detection (LOD) and limits of quantification (LOQ) of the analytes determined.

Analytes	Method LOD (pmol m^{-3})	Method LOQ (pmol m^{-3})	% RSD ($n = 6$)	Accuracy	
				40 ng mL^{-1}	200 ng mL^{-1}
Xylose	0.05	0.16	14.5	42.0	181
Arabinose	0.08	0.28	9.0	34.7	212
Rhamnose	0.04	0.13	21.2	34.9	217
Fucose	0.07	0.22	15.7	38.6	218
Glucose + Mannose	0.05	0.15	19.3	33.8	180
Galactose	0.05	0.18	13.7	31.2	178

$2\text{--}6\text{ m s}^{-1}$ range and seldom $> 10\text{ m s}^{-1}$, and confined to the synoptically active period in the beginning of the expedition.

The advection of air masses during the course of the PI-drift was typical for the central Arctic in summer (Fig. 2a). The air that originated from the open seas surrounding the central Arctic dominated. In agreement with earlier high Arctic summer studies, air either from continents or subsiding from the free troposphere was of much less importance (Bigg et al., 1996, 2001; Leck and Persson, 1996a). The backward trajectories shown in Fig. 2b–e were for the PI-drift subjectively classified in four clusters depending on their geographical origin. The origin of the air during both the 1st (DOY 227, DOY 229–232) and 2nd (DOY 228, DOY 236, 238–239) clusters was highly variable on a daily basis as of the very synoptically active period during the first half of the expedition. The air of cluster 1 (Fig. 2b) originated easterly from the Barents and Kara seas. For cluster 2 (Fig. 2c), they came from the Fram Strait – Greenland Sea area. In both clusters the air spent a relatively short time over the ice (DOI ~ 2) since last contact with open sea. The air origin during the 3rd cluster (DOY 234–235) was mainly from Greenland (Fig. 2d). The vertical component of the air trajectories (not presented) shows a subsiding pathway from the free troposphere across Greenland to the surface, which suggests that the air sampled onboard *Oden* was of free-tropospheric origin. As in this case the trajectories did not have any contact with the open sea, no DOI could be calculated. During DOY 240–246 (4th cluster, Fig. 2e) the air flow was largely from the northwestern circumpolar region over the pack ice for approximately DOI = 8 and from the direction of the Laptev and East Siberian seas towards the end of the period but still with no close contact with open sea. During the OW1 and MIZ1 (DOY 216–218) we experienced air predominantly from the ice-covered archipelago north of Canada and Alaska, whereas during MIZ2 and OW2 the air came from Kara Sea area with possible adjoining land contact.

Surface air temperatures varied substantially from near 0°C to -12°C but were observed mostly in the -2 to 0°C interval. The colder temperatures prevailed in a brief episode and in a period appearing towards the end of August. The analyses of the surface energy budget at the location of the

ship (Sedlar et al., 2011) allowed for a division of the PI-drift into four separate regimes (R): (1) (R1) DOY 226 to DOY 233 (dominated by the 1st trajectory cluster) had numerous melt ponds on the ice surface, with temperatures around 0°C ; (2) the melt was followed by (R2) with a drop in temperature to -6°C for about 2.5 days (DOY 234 to DOY 237 including the 3rd trajectory cluster); (3) the conditions in (R3) DOY 240 to DOY 243 were governed by a persistent stratocumulus layer that contributed to maintaining the temperatures between -2 and -3°C ; and (4) (R4) started on 31 August (DOY 244) and ended on September 2 (DOY 246) as the persistent stratocumulus layer went away and the clouds, if present, became optically thin (Mauritsen et al., 2011), which resulted a drastic drop in temperature to -12°C and sunny conditions. The 2nd trajectory cluster, depicted in Fig. 2c, represents a minor part of R1 and the period during the transition between R2 and R3. To account for differences in the meteorological conditions encountered between R3 and R4, we divided the 4th trajectory cluster (Fig. 2e) into two sub-clusters, Fig. 2f (DOY 240–243) and Fig. 2g (DOY 244–246).

In order to fully understand the availability of the gel particles derived from bubble bursting at the seawater surface, their possible enrichment in the SML also needs to be confirmed. In a parallel study during ASCOS (Gao et al., 2012), it was proposed that bubble scavenging of surface-active polysaccharides was one of the possible mechanisms for the observed enrichment of polysaccharides in the SML located at the air–sea interface. Gao et al. (2012) also observed that newly released gel polymers from sea ice algae were more favorably scavenged into the SML, which is consistent with the idea that the porous nature of sea ice not only provides a habitat for ice algae but also opens a pathway for exchanges of organic matter with the seawater below. The authors concluded that the melting sea ice containing high standing stocks of microalgae and bacteria elevated the input of polymer gels into seawater and subsequently enhanced the enrichment of polysaccharides in the SML at the air–sea interface. According to Gao et al. (2012) the same processes promoting the formation of SML polymer gels and their saccharides would also apply in the MIZ.

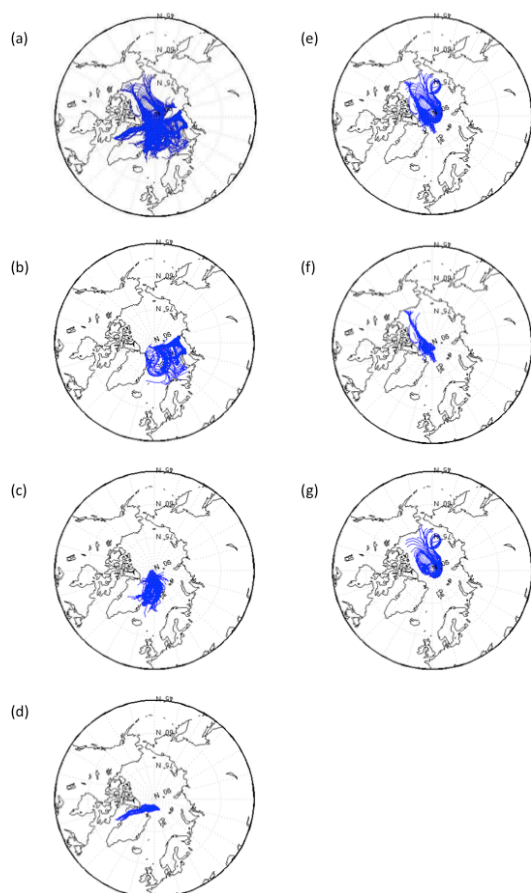


Fig. 2. Backward trajectory clusters with an arrival height of 100 m at the position of the icebreaker during (a) the ice drift (PI-drift), (b) cluster 1 (DOY 227, DOY 229–232) originated easterly from the Barents and Kara seas, (c) cluster 2 (DOY 228, DOY 236, 238–239) from the Greenland Sea–Fram Strait area, (d) cluster 3 (DOY 234–235) from Greenland, (e) cluster 4 (DOY 240–246) from the northwestern circumpolar region over the pack ice, (f) sub-cluster 4a (DOY 240–243), and (g) sub-cluster 4b (DOY 243–246).

5 Atmospheric particulate mass concentrations of hydrolyzed polysaccharides

5.1 Concentrations shown as total, sub- and super-micrometer size fractions

Table 2 gives basic descriptive statistics of all monosaccharides (hydrolyzed polysaccharides) measured during the expedition. The data is shown separately for open water (OW 1,2), marginal ice zone (MIZ 1,2) and pack ice (PI-drift) measurements. The mass determinations of the 5 BCI stages were grouped to approximately represent the sub-micrometer diameter range (sum of stage 1 and 2, 0.035–0.665 μm) and the super-micrometer range (sum of stage 3, 4 and 5, 0.665–10 μm). For the samples collected during the PI-drift the 25th, 50th (median) and 75th percentile values of the relative abundance of both THNS and the various

monosaccharides were additionally calculated. Table 2 also tabulates detection frequencies for both THNS and the individual monosaccharides. The temporal variability of THNS in the grouped BCI data are depicted in Fig. 3.

In the Greenland Sea–Fram Strait area, concentrations of THNS summed over all BCI stages (0.035–10 μm) ranged from about 225 pmol m^{-3} (OW1) and 189 pmol m^{-3} (MIZ1) in August to about 129 pmol m^{-3} in (OW2) and 111 pmol m^{-3} (MIZ2) in September. For the PI-drift a weak trend was observed with slightly elevated median concentrations measured for R1 and R2 (46 pmol m^{-3}) compared with R3 and R4 (25 pmol m^{-3}). Period R2 was relatively colder, with leads starting to freeze on DOY 233, with a layer of frazil ice, until DOY 238, when (R3) the lead opened up, exposing open water again for the final lead freeze-up at the end of R4. In September both the OW and MIZ concentrations of THNS had declined by about 45 %, within 6 weeks. All monosaccharides determined from the polysaccharide hydrolyses were lowest in concentrations in air masses that had spent more than 5 days over the pack ice area since last contact with open sea (discussed further in Sect. 6). The above results are not only consistent with the relatively more biologically active waters of the Greenland Sea–Fram Strait area (Leck and Persson, 1996a, b; Gao et al., 2012) but also consistent with observations of the aerosol source strength based on the eddy-covariance flux measurements during ASCOS (Held et al., 2011a) and during a similar expedition to the same area and season during 1996 (Nilsson et al., 2001), which showed an order of magnitude stronger flux of bubble-bursting aerosol particles over the open sea than from open leads.

The temporal variability in the grouped BCI data (Fig. 3) appeared in general similar in the sub- and super-micrometer particles. However, episodically a remarkable gradient in concentrations was observed during DOY 238 to 245 with a minimum on DOY 242. The THNS concentrations in the super-micrometer subset varied considerably over 2 orders of magnitude, ranging from 1.1 to 157.4 pmol m^{-3} . The THNS concentrations in sub-micrometer particles exhibited slightly less variability, ranging from 4.3 to 138.4 pmol m^{-3} . For samples collected during the PI-drift a sub-micrometer to total THNS median molar ratio of 53 % was calculated. The samples collected in the Greenland Sea–Fram Strait area on the outward transit exhibited a corresponding molar ratio of 73 % for MIZ2 and 66 % for OW2, whereas those collected during OW1 and MIZ1 showed lower ratios (both 39 %). Among the seven targeted analytes, xylose and glucose + mannose were the predominant monosaccharides (detection frequency > 80 %), accounting for over 63 % (mole %) of the combined mass of monosaccharides determined.

5.2 Mass median size distributions

From the size distribution (5-stage BCI) data, the 25th, 50th (median), and 75th percentile values of monosaccharides

Table 2. Monosaccharide composition of size-resolved aerosol particles collected during ASCOS.

Station	Sampling period in DOY (no. of samples)	Size range ^a	THNS, pmol m ⁻³	% Sub-micrometer mass to the mass of total (THNS)	Monosaccharide composition, %					
					Xylose	Arabinose	Rhamnose	Fucose	Glucose + Mannose	Galactose
OW1	216.561–217.342 (1)	Sub	88.3	39.2	36.9	2.9	8.0	2.0	36.3	13.9
		Super	137.0		25.3	6.3	33.4	n.d. ^b	20.2	14.9
MIZ1	217.503–218.508 (1)	Sub	73.0	38.6	55.2	2.3	8.7	n.d.	26.6	7.2
		Super	116.0		33.0	2.4	0.3	1.3	56.5	6.4
PI-drift	225.967–245.952 (14)	Sub								
		Median	24.8	53.0 (34.0, 69.6) ^c	32.0	3.8	10.8	0.4	47.1	6.3
		25th percentile	11.7		17.1	2.3	6.1	0.1	33.4	3.1
		75th percentile	26.9		36.8	5.2	23.3	2.0	56.3	8.3
		Super								
		Median	12.7		28.0	1.2	3.3	1.6	52.5	7.8
		25th percentile	7.3		22.6	n.d.	1.4	0.2	32.8	1.7
75th percentile	28.7		39.4	3.2	4.5	4.2	63.9	12.9		
MIZ2	250.468–251.091 (1)	Sub	81.6	73.4	82.9	55.7	45.7	42.9	92.8	60.1
		Super	29.6		49.4	n.d.	7.0	n.d.	36.4	7.2
OW2	251.181–251.666 (1)	Sub	84.8	65.8	59.9	3.7	5.6	n.d.	28.4	2.3
		Super	44.1		35.7	1.9	24.3	n.d.	38.2	n.d.
					18.2	1.7	2.4	n.d.	63.6	n.d.

^a Particles in the (sub)-micrometer size range (sum of BCI stage 1 and 2, 0.035–0.665 μm) and (super)-micrometer size range (sum of BCI stage 3, 4 and 5, 0.665–10 μm).

^b n.d. = the value is below detection limit.

^c The values indicated in the parenthesis represent 25th and 75th percentile value of the % Sub- to THNS.

^d % D.F. = % detection frequency.

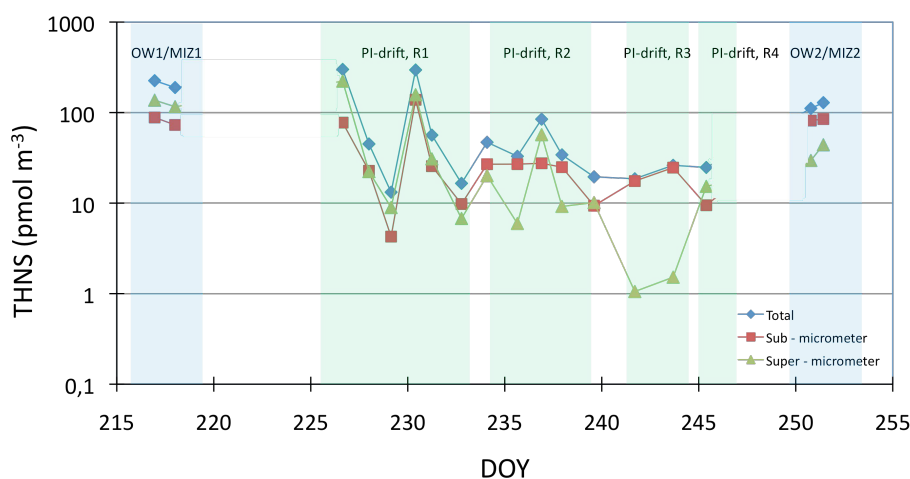


Fig. 3. Temporal variation of particulate THNS (total hydrolysable neutral sugar) mass concentration (pmol m⁻³), grouped in the sub- and super-micrometer size ranges. The division into four separate regimes (R1–4) during ice drift (PI-drift: DOY 225–245), based on the analyses of the surface energy budget (see Sect. 4.1 for details), is indicated by light-green panels. The inward and outward OW and MIZ stations are indicated by light-blue panels. The thin line connecting the subsequent samples is inserted to help the eye to separate the three categories of THNS (total, sub-micrometer, super-micrometer).

grouped into three categories (*pentoses*: xylose and arabinose; *hexoses*: glucose, mannose and galactose; and *deoxysugars*: rhamnose and fucose) were calculated for the OW1,2 (number of samples $n = 2$), MIZ1,2 ($n = 2$) and PI-drift ($n = 14$) subsets, respectively. The result is presented in Fig. 4. The large span observed for the three subsets (OW/MIZ/PI-drift) implied that there was a high degree of spatial and temporal variability in the mass concentrations resolved over size. Also the small number of samples available in the Greenland Sea–Fram Strait area probably biases the uncertainty measure in the waters along the ice edge.

Size distributions of deoxysugars were clearly bimodal both over the pack ice and in the Greenland Sea–Fram Strait area, with PI-drift 70 ± 30 (1σ)%, MIZ 81 ± 13 (1σ)% and OW 94 ± 11 (1σ)% of the mass occurring in the Aitken mode (stage 1, 0.035–0.665 μm). Close to half (43%) of the pentose and hexose size distributions observed over the pack ice showed also a bimodal character, but less pronounced, with peak concentrations frequently associated with the coarse mode (stage 4, 2.12–5.0 μm). Relative to the deoxysugars a larger fraction of their sub-micrometer mass was in the accumulation mode (stage 2, 0.161–0.665 μm):

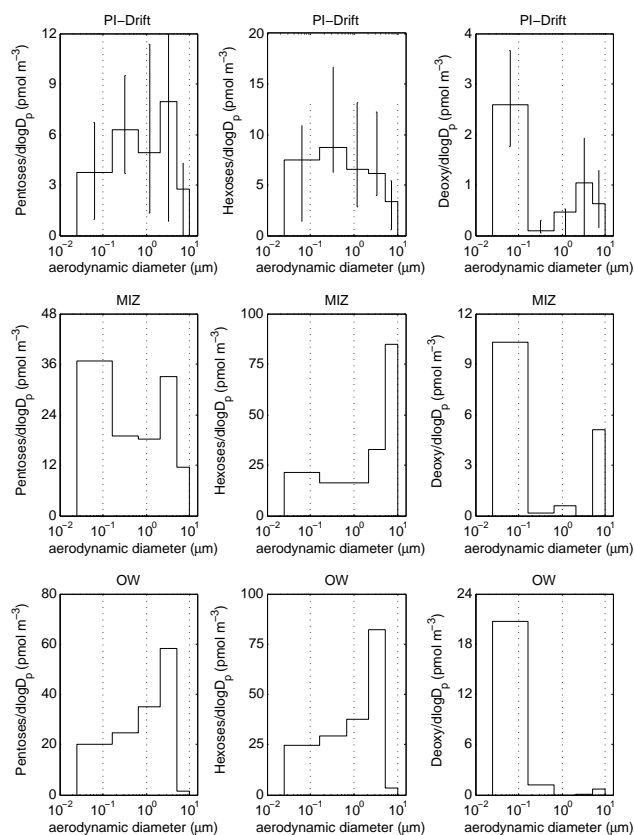


Fig. 4. Size distribution of particulate pentoses, hexoses and deoxy-sugars collected over the pack ice during the PI-drift (upper panel), at the MIZ (middle panel), and in the OW (lower panel). Error bars indicate the 25th and 75th percentile values.

pentose 24 ± 25 (1σ)% and hexose 13 ± 22 (1σ)%. The corresponding numbers for the sum of the Aitken and accumulation modes (stage 1 + 2, 0.035 – 0.665 μm) were pentose 52 ± 33 (1σ)% and hexose 63 ± 39 (1σ)%. The observed size distributions of hexoses in the MIZ of the Greenland Sea–Fram Strait area showed a similar but weak bimodal character, with 37 ± 33 (1σ)% of the mass occurring in the sum of the Aitken and accumulation modes. For pentose the maximum sub-micrometer concentration was, however, more distinctly associated with the smallest particles: (Aitken mode) 45 ± 17 (1σ)%. For the samples collected over the Greenland Sea (OW1,2) peak mass concentrations for the pentose and hexose monomers were found in the largest size fractions, with at least 55 ± 23 (1σ)% associated with the coarse mode (stage 3, 4 and 5, 0.665 – 10 μm). In general for the samples collected over the pack ice, peak levels for coarse-mode mass, for all three categories, occurred interestingly in the middle size fraction (stage 4, 2.12 – 5.0 μm). This would tend to indicate a gradual removal of the jet-drop-sized aerosol particles sourced from the open sea and ice edge zone as the air passes over the pack ice. Nilsson and Bigg (1996) and Leck et al. (2002) observed a high fre-

quency of stratiform clouds accompanied by advection fogs during transport of air from open sea to pack ice. The ensuing efficient wet removal combined with a weak particle source strength (Held et al., 2011a, b), causally related to the typically low winds (< 6 m s^{-1}) and to the modest extent of open leads, could have accounted for a significant loss of large particles. To some extent this feature was also indicated in the MIZ samples collected in foggy conditions.

Deoxysugars have frequently been detected in phytoplankton exudates and in non-photosynthetic microbial (i.e., bacteria) polysaccharides (Mopper et al., 1995; Zhou et al., 1998). Deoxysugars in seawater usually occur in elevated levels due to their slow rate of degradation relative to that of other sugar units of the polymer gel composition (Giroldo et al., 2003). According to other studies of seawater, the abundant glucose + mannose (hexoses) and xylose (pentose) in the samples collected could be associated with the cellular materials of phytoplankton, and thus belong to the family of structural and/or storage polysaccharides (i.e., xyloglucan, glucan or glycoprotein) (Panagiotopoulos and Sempere, 2005; Skoog and Benner, 1998). It is also possible for these sugars to be part of the major components of bioavailable polysaccharides and thus to be easily degraded via microbial utilization into oligosaccharides and subsequently to monomers in free form. The hexose monomer content of the accumulation and coarse modes during this study could therefore not only result from dissolved organic matters (mainly glucose) but also from phytoplankton exudates similar to the deoxysugars.

5.3 Comparison with other studies

As this is a novel study, with first-time determination of naturally occurring polysaccharides in size-resolved atmospheric aerosols, direct comparisons with other measurements are not possible. Instead, an indirect comparison utilized the reported levels from a parallel study during ASCOS, the determined organics in the marine sub-micrometer aerosol in air by Chang et al. (2011), using an aerosol mass spectrometer. Chang et al. (2011) reported a sub-micrometer organic mass of about 0.055 $\mu\text{g m}^{-3}$. Gao et al. (2012) estimated the fraction of THNS to be about 1.5 – 3 % (2.7 % on average) of the organic matter dissolved in surface seawater during ASCOS. By assuming the same fraction of THNS in atmospheric organic particulate matters, the THNS in the organic aerosols studied by Chang et al. (2011) would correspond to the order of 10 pmol m^{-3} THNS. This is comparable to our results, with a measured mass concentration of THNS between 16 and 43 pmol m^{-3} (between the 25th and 75th percentiles).



Fig. 5. Median THNS mass concentrations (pmol m^{-3}) of particles in the sub-micrometer (blue) and super-micrometer (red) size ranges, calculated for in trajectory cluster 1, 2, 4a and 4b, respectively.

6 Changes in hydrolyzed polysaccharides in relation to changes in source strength, long-range advection, and vertical mixing

6.1 Changes over the four regimes

The four regimes encountered during the PI-drift are indicated in Fig. 3. Regime 1 (DOY 226 to 233) was dominated by air masses (Fig. 2b) originating from the eastern sector towards Barents and Kara seas having spent a relative short time (DOI = 2 days) spent over the pack ice. Within this trajectory cluster the THNS mass concentrations of the particles collected at the position of the ship (about 87° N) were highest, having approximately with two thirds of the mass within the Aitken plus accumulation modes (Fig. 5). On DOY 231 a significant enhancement of THNS was observed in the both the sub- and super-micrometer size range (Fig. 3).

Calculated super-micrometer Cl^-/Na^+ molar ratios in parallel BCI samplers onboard ship (Leck, unpublished data), resulted in a molar ratio of circa 1.0 (DOY 230), which indicated very recent sea-salt production from jet drops (Leck et al., 2002). Even if the jet drop particles were mainly composed of sea salt, their past observed coating of highly surface-active polymer gels (Leck et al., 2002) is suggested to explain the observed high super-micrometer THNS mass concentrations. A similarly active film drop mode would explain the sub-micrometer mass enhancements.

The samples collected with the 2nd trajectory cluster, depicted in Fig. 2c, (minor part of R1 and during the transition between R2 and R3) were influenced by air masses from the Greenland Sea–Fram Strait area around 2 days prior. Average THNS mass concentrations measured (Fig. 5) were about 70 % lower in the super-micrometer fraction relative to the sub-micrometer size fraction. When compared with the 1st trajectory cluster, no significant change of the sub-micrometer THNS mass concentration was observed. Based on previous studies (Heintzenberg et al., 2006; Heintzenberg

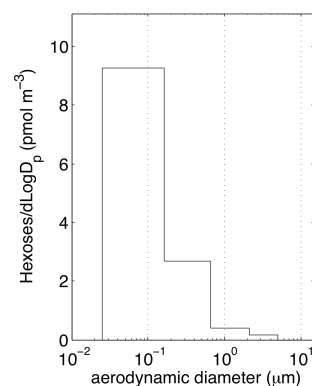


Fig. 6. Mass size distribution of particulate hexose monomers for trajectory cluster 4a during R3.

and Leck, 2012; Nilsson and Leck, 2002) one possible cause of the less pronounced super-micrometer mass fraction is the efficient wet deposition through drizzle from fog and low cloud, common in the marginal ice zone, as relatively warm moist air is advected in over the pack ice while being saturated by cooling from the surface. However, such conditions could equally have applied to the 1st trajectory cluster (Fig. 2b). Another perhaps more relevant cause relates to the reduced synoptic activity encountered, during the 2nd cluster, and the expected lower surface wind speeds at the MIZ/open water. According to Leck et al. (2002), such conditions would have resulted in a weaker flux of jet drops with subsequent lower mass apportioned in the super-micrometer size fraction.

To be able to view the distribution in the measured THNS data between R3 and R4, we divided the samples collected within the 4th trajectory cluster into two sub-clusters. They are pictured in Fig. 2f (cluster 4a, DOY 240–243) and g (cluster 4b, DOY 244–246), and represent air that spent ca. 7 days or more over the pack ice. Compared with cluster 1 and 2, a general decrease in THNS mass concentrations is observed, with increasing length of time spent over the pack ice since last contact with open sea. This is consistent with previous results over the central Arctic Ocean by Heintzenberg et al. (2006) and during ASCOS (Heintzenberg and Leck, 2012) based on modal statistics of aerosol concentration by number.

The comparably high THNS levels in the sub-micrometer size range together with the very low THNS mass fraction in the super-micrometer part of the samples collected during R3 (cluster 4a) needs to be further investigated. The very strong predominance of the mass of hexoses in the Aitken mode, shown in Fig. 6, stands out when comparing the BCI size distributions measured within R3 with the statistics of all samples collected during PI-drift (Fig. 4).

Figure 7 shows a comparison of the median relative mass contribution of the monosaccharides determined in the Aitken mode of cluster 4a (Fig. 7a) with the median

relative mass contribution to the sub-micrometer aerosol collected during the PI-drift (Fig. 7b). A study of Panagiotopoulos and Sempere (2005) showed that dissolved particulate matter in seawater, from various locations, can be distinguished by their monosaccharide composition. The corresponding relative mass distribution of the nascent aerosol is shown in Fig. 7c. As the nascent particles were in situ generated by artificial bubble bursting at the open lead site adjacent to the drifting ice floe, their monosaccharide fingerprint should be specific for material from the lead surface waters. The higher sub-micrometer mass contribution of glucose + mannose (78 %) collected during DOY 242 (Fig. 7a), relative to what was found both in the nascent particles and in general for the sub-micrometer aerosol collected during PI-drift (Fig. 7b; 41 % on average), indicated that the air masses sampled onboard ship had likely been in contact with continental combustion sources (Carvalho et al., 2003; Tominaga et al., 2011): cellulose is the macro-polymer of glucose and will decompose to its monomer at temperatures above 300 °C. Glucose is therefore used as a tracer (among others) for combustion sources. As discussed in Sect. 3.2 the air sampled at 25 m above sea level was in general confined to a well-mixed surface-based layer. However during DOY 242 our sampling coincided with the re-coupling and turbulent mixing between a shallow (~150 m deep) surface-based mixed layer and with a separate mixed layer located in the upper part of the boundary layer – the upper half of which contained stratocumulus clouds. This re-coupling can be clearly identified in radiosonde and turbulence profiles from a tethered balloon (Shupe et al., 2013). Backward-trajectory analysis suggests that the air in the upper-boundary layer had come from the Canadian Arctic Archipelago while that in the lowest 100 m had been over the ice for at least 10 days. Based on the hexose fingerprint we therefore speculate that the surface air that mixed with the upper part of the boundary layer was influenced by continental sources. The Chang et al. (2011) results from ASCOS also lend strong support to the air originating from continental combustion sources, since elevated levels of acetonitrile (combustion of biomass) and ^{210}Pb (a continental tracer) were observed.

6.2 Changes since last time in contact with open sea

It has become clear from the above discussion that understanding chemical transformations in the atmosphere over the pack ice, which will shape the observed polysaccharide subunit monomer mass size distributions at the location of the ship, will also require an understanding of the synoptic-scale systems advecting heat, moisture, and particles from the surrounding open seas for a variable length of time over the pack ice. In Fig. 8 we utilized the travel time over ice since last contact with open sea, DOI, as a simple parameter to summarize the evolution of the atmospheric polymer gel, with its sugar composition divided into three classes (THNS, structural or cellular materials of phytoplankton: pentoses,

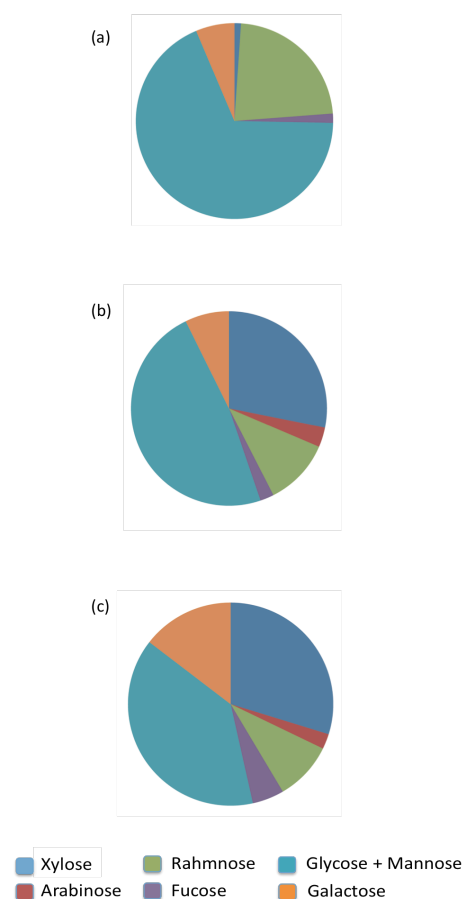


Fig. 7. Relative percentage of monosaccharides determined (a) in the Aitken and accumulation mode (BCI stage 1 and 2, 0.035–0.665 μm) during DOY 242 (a sample most likely influenced by continental combustion sources); (b) during the PI-drift, Aitken and accumulation mode (BCI stage 1 and 2, 0.035–0.665 μm); and (c) from bubble-generated sea spray aerosol at open lead site (<1 μm).

hexoses, and extracellular deoxysugars). When the trajectories did not have any contact with the open sea, no DOI was calculated. Corresponding samples are not included in Fig. 8. Thus the samples included in Fig. 8 all have a common source area in the open water south of or at the MIZ with no contact with other sources but marine as the air was advected for various length of time in over the pack ice area.

For the extracellular deoxysugars (Fig. 8, light blue) no significant change in the apportioned mass in the sub-micrometer size range (Aitken and accumulation modes) as a function of travel time over ice (DOI) was seen. Close to the ice edge and after travel times up to two days, however, a decline is weakly indicated for the all classes. Beyond DOI = 5 both the THNS (Fig. 8 dark grey) and pentose/hexose (Fig. 8 red) classes show a significant relative increase in the sub-micrometer size range. Also for travel times of five days and longer both the structural and extracellular sugars in the

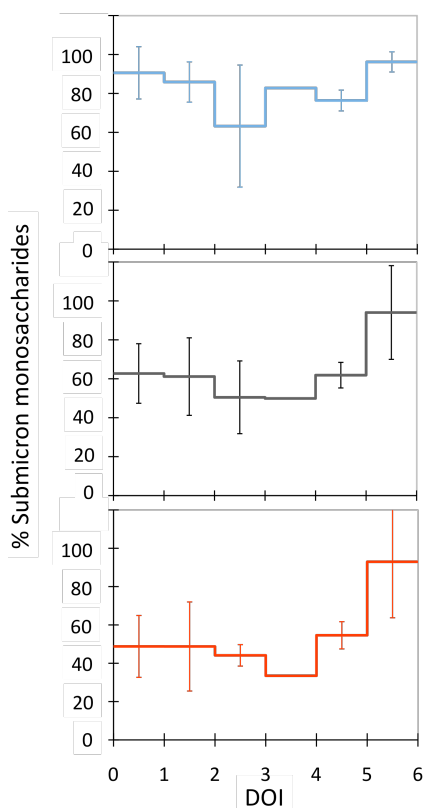


Fig. 8. Relative sub-micrometer (Aitken and accumulation mode) to total mass (%), of deoxy-sugars (light blue), THNS (dark grey), and the sum of pentoses and hexoses (red) as a function of travel time over ice (DOI). Data for all travel times of five days and longer have been collected in the column 5–6 days. Error bars indicate $\pm 1\sigma$. For $3 < \text{DOI} < 4$, $n = 1$.

sub-micron particles dominate the total mass of sugars in all particle sizes (close to 90 %).

6.3 The relevance of polymer gels for cloud activation

In the atmosphere, transformations of polymer gels will occur due to exposure of UV light, which has been shown to shorten their polysaccharide chains into smaller units that cannot reassemble (Orellana and Verdugo, 2003). Thus the mass of the primary polymer gel particles will be conserved but divided into smaller units. These are processes that would be promoted with cloud processing and long travel times over the pack ice and would serve as a potential for the atmospheric polymer gels, with their partially colloidal (extracellular) and granular (structural) structures, to separate into colloidal fragments having sizes within the sub-accumulation mode peaking in the Aitken mode around 40 nm in diameter (Leck and Bigg, 2005a, 2010; Orellana et al., 2011). The results of this study are consistent with such a transformation, which is indicated by in the relatively high abundance of extracellular deoxy-sugars in the Aitken mode (Fig. 4) in

air being advected over the pack ice. It is also possible that the relative high presence of structural sugars, e.g., glucose (hexoses), for advection times of 5 days or longer over the ice, could have resulted from phytoplankton exudates.

In an attempt to explain the characteristics of “colloidal fragmentation” of polymer gels in the high Arctic, a hypothesis has been put forward linking it to evaporation of cloud – or fog – droplets by mixing with air, low in moisture, at the top and edges of a cloud/fog (Karl et al., 2013; Leck and Bigg, 1999, 2010), whereby the colloidal fragments would be released during evaporation.

Moreover, the relatively high abundance of extracellular deoxy-sugars in the Aitken mode in air being advected over the pack ice is indicative of the presence of highly surface-active constituents (Gao et al., 2012) promoting cloud droplet activation of polymer gels (Ovadnevaite, 2011). The polysaccharide subunit monomer mass of the Aitken mode particles, observed in this study, associated with the gels found in the open lead surface microlayer (Gao et al., 2012) could thus be important for cloud droplet formation over the inner summer Arctic. Thus, the findings in this study are consistent with the recent study by Orrelana et al. (2011), which strongly advocated that marine microgels dominate the available CCN number population in the high Arctic (north of 80° N) during the summer season.

7 Conclusions

Novel use of the LC–MS–MS technique provided the first quantitative determination of marine biogenic polysaccharides and their subunit monomers in size-resolved atmospheric particles. It has strengthened the quantitative information on the contribution of polymer gels to the ocean-derived marine aerosol in the atmosphere compared with earlier methods (Facchini et al., 2008; Kuznetsova et al., 2005; Leck and Bigg, 2005a; Hawkins and Russell, 2010; Orellana, 2011; Posfai et al., 2003; Russell et al., 2010).

The size-resolved data showed a distinctive feature of heteropolysaccharides, enriched in the pentose xylose, hexoses glucose + mannose as well as a substantial fraction of deoxy-sugars (rhamnose and fucose).

From 3 August to 8 September 2008, THNS mass concentration within the super-micrometer particle size range varied over 3 orders of magnitude ($1\text{--}160\text{ pmol m}^{-3}$) and to a slightly lesser extent in the sub-micrometer particles ($4\text{--}140\text{ pmol m}^{-3}$). The highest THNS values were observed in the open waters and along the ice edge zone of the Greenland Sea–Fram Strait area, in August. In September both the OW and MIZ concentrations had declined by about 45 %. For all monosaccharides investigated the lowest concentrations were found in air masses that had spent more than 5 days over the pack ice area since last contact with open sea. A possible explanation is the more biologically active waters of the Greenland Sea–Fram Strait area and the much stronger

flux of bubble-bursting aerosol over the open sea than from open leads. For samples collected during the PI-drift on average $53 \pm 24\%$ of the THNS was apportioned in the Aitken and accumulation mode, increasing to more than 90% with a longer period of time ($\text{DOI} > 7$ days) spent over the pack ice.

The mass size distributions of extracellular deoxysugars exhibited a clear bimodal structure with peak concentrations in the Aitken mode both in samples collected during the PI-drift and during the MIZ/OW stations, whereas the structural sugars, pentoses and hexoses, showed a less pronounced bimodal character, with peak concentrations frequently associated with the course mode.

The similarity in monosaccharide fingerprint between the ambient aerosol and those in situ generated at the open lead site lends support to the suggestion that bubble bursting is capable of providing the Aitken and accumulation mode particles originating from marine polymer gels. We speculate that there is a potential for the polymer gels, with their partially colloidal (extracellular) and granular (structural) structures and with time spent in the air, to separate into fragments after exposure to ultraviolet light and subsequent release of particles during evaporation as has been suggested by Leck and Bigg (1999, 2010). This was indicated in samples representing advection times of five days and longer where both the structural and extracellular sugars in sub-micrometer particles dominated the total mass of sugars in all particle sizes (close to 90%).

The occurrence of atmospheric surface-active polymer gels with their hydrophilic and hydrophobic segments (Orellana et al., 2011; Xin et al., 2013), as demonstrated in this study, suggests that marine polymer gels could potentially become important for cloud droplet activation over the inner summer Arctic with possible influence on the melting and freezing of the perennial sea ice. It is hoped that this possibility (whether it turns out to be significant or not) will renew interest in the complex but fascinating interactions between marine microbiology, aerosol, clouds and climate.

Acknowledgements. We thank L. Orr for providing the back trajectories. M. Karl's and J. Heintzenberg's comments on an early version of the article are appreciated. This work is part of ASCOS (the Arctic Summer Cloud Ocean Study). ASCOS was made possible by funding from the Knut and Alice Wallenberg Foundation and the DAMOCLES European Union 6th Framework Programme Integrated Research Project. The Swedish Polar Research Secretariat (SPRS) provided access to the icebreaker *Oden* and logistical support. M. Tjernström is specifically thanked for his co-coordination of ASCOS. We are grateful to the SPRS logistical staff and to *Oden's* Captain Mattias Peterson and his crew. ASCOS is an IPY project under the AICIA-IPY umbrella and an endorsed SOLAS project. Support for this work was provided by the Swedish Research Council (VR) and the Knut and Alice Wallenberg Foundation.

Edited by: I. Brooks

References

- Berner, A., Luzer, C., Pohl, F., Preining, O., and Wagner, P.: The size distribution of the urban aerosol in Vienna, *Sci. Total Environ.*, 13, 245–261, 1979.
- Bigg, E. K.: Comparison of aerosol at four baseline atmospheric monitoring stations, *J. Appl. Meteorol.*, 19, 521–533, 1980.
- Bigg, E. K.: Sources, nature and influence on climate of marine airborne particles, *Environ. Chem.*, 4, 155–161, 2007.
- Bigg, E. K. and Leck, C.: Cloud-active particles over the central Arctic Ocean, *J. Geophys. Res.*, 106, 32155–32166, 2001.
- Bigg, E. K. and Leck, C.: The composition of fragments of bubbles bursting at the ocean surface, *J. Geophys. Res.*, 113, D11209, doi:10.1029/2007JD009078, 2008.
- Bigg, E. K., Leck, C., and Nilsson, E. D.: Sudden changes in arctic atmospheric aerosol concentrations during summer and autumn, *Tellus B*, 48, 254–271, 1996.
- Bigg, E. K., Leck, C., and Nilsson, E. D.: Sudden changes in aerosol and gas concentrations in the central Arctic marine boundary layer: Causes and consequences, *J. Geophys. Res.*, 106, 32167–32185, 2001.
- Bigg, E. K., Leck, C., and Tranvik, T.: Particulates of the surface microlayer of open water in the central Arctic Ocean in summer, *Mar. Chem.*, 91, 131–141, 2004.
- Blanchard, D. C.: The Oceanic Production of Volatile Cloud Nuclei, *J. Atmos. Sci.*, 28, 811–812, 1971.
- Blanchard, D. C. and Syzdek, L. D.: Film Drop Production as a Function of Bubble Size, *J. Geophys. Res.*, 93, 3649–3654, 1988.
- Blanchard, D. C. and Woodcock, A. H.: Bubble formation and modification in the sea and its meteorological significance, *Tellus*, 9, 145–148, 1957.
- Carvalho, A., Pio, C., and Santos, C.: Water-soluble hydroxylated organic compounds in German and Finnish aerosols, *Atmos. Environ.*, 37, 1775–1783, 2003.
- Chang, R. Y.-W., Leck, C., Graus, M., Müller, M., Paatero, J., Burkhardt, J. F., Stohl, A., Orr, L. H., Hayden, K., Li, S.-M., Hansel, A., Tjernström, M., Leaitch, W. R., and Abbatt, J. P. D.: Aerosol composition and sources in the central Arctic Ocean during ASCOS, *Atmos. Chem. Phys.*, 11, 10619–10636, doi:10.5194/acp-11-10619-2011, 2011.
- Chin, W.-C., Orellana, M. V., and Verdugo, P.: Spontaneous assembly of marine dissolved organic matter into polymer gels, *Nature*, 391, 568–572, 1998.
- Covert, D. S., Widensohler, A., Alto, P., Heintzenberg, J., McMurry P. H., and Leck, C.: Aerosol number size distributions from 3 to 500 nm diameter in the arctic marine boundary layer during summer and autumn, *Tellus B*, 48, 197–212, 1996.
- Decho, A. W.: Microbial exopolymer secretions in ocean environments: Their role(s) in food webs and marine processes, *Oceanogr. Mar. Biol.*, 28, 73–153, 1990.
- Draxler, R. R. and Rolph, G. D.: HYSPLIT (HYbrid Single-Particle Lagrangian Integrated Trajectory) Model access via NOAA ARL READY Website (<http://ready.arl.noaa.gov/HYSPLIT.php>), NOAA Air Resources Laboratory, Silver Spring, MD, 2011.
- Facchini, M. C., Rinaldi, M., Decesari, S., Carbone, C., Finessi, E., Mircea, M., Fuzzi, S., Ceburnis, D., Flanagan, R., Nilsson, E. D., de Leeuw, G., Martino, M., Woeltjen, J., and O'Dowd, C. D.: Primary submicron marine aerosol dominated by

- insoluble organic colloids and aggregates, *Geophys. Res. Lett.*, 35, L17814, doi:10.1029/2008GL034210, 2008.
- Gao, Q., Araia, M., Leck, C., and Emmer, A.: Characterization of exopolysaccharides in marine colloids by capillary electrophoresis with indirect UV detection, *Anal. Chim. Acta*, 662, 193–199, 2010.
- Gao, Q., Nilsson, U., Ilag, L. L., and Leck, C.: Monosaccharide compositional analysis of marine polysaccharides by hydrophilic interaction liquid chromatography-tandem mass spectrometry, *Anal. Bioanal. Chem.*, 399, 2517–2529, 2011.
- Gao, Q., Leck, C., Rauschenberg, C., and Matrai, P. A.: On the chemical dynamics of extracellular polysaccharides in the high Arctic surface microlayer, *Ocean Sci.*, 8, 401–418, doi:10.5194/os-8-401-2012, 2012.
- Gershey, R. M.: Characterization of seawater organic matter carried by bubble-generated aerosols, *Limnol. Oceanogr.*, 28, 309–319, 1983.
- Giroldo, D., Vieira, A., and Paulsen, B.: Relative increase of deoxy sugars during microbial degradation of an extracellular polysaccharide released by a tropical freshwater *Thalassiosira SP*, *J. Phycol.*, 39, 1109–1115, 2003.
- Gras, J. L. and Ayers, G. P.: Marine aerosol at southern midlatitudes, *J. Geophys. Res.*, 88, 10661–10666, 1983.
- Hawkins, L. N. and Russell, L. M.: Polysaccharides, Proteins, and Phytoplankton Fragments: Four Chemically Distinct Types of Marine Primary Organic Aerosol Classified by Single Particle Spectromicroscopy, *Advances in Meteorology*, 2010, 612132, doi:10.1155/2010/612132, 2010.
- Heintzenberg, J. and Leck, C.: The summer aerosol in the central Arctic 1991–2008: did it change or not?, *Atmos. Chem. Phys.*, 12, 3969–3983, doi:10.5194/acp-12-3969-2012, 2012.
- Heintzenberg, J., Leck, C., Birmili, W., Wehner, B., Tjernström, M., and Wiedensohler, A.: Aerosol number-size distributions during clear and fog periods in the summer high Arctic: 1991, 1996 and 2001, *Tellus B*, 58, 41–50, 2006.
- Held, A., Brooks, I. M., Leck, C., and Tjernström, M.: On the potential contribution of open lead particle emissions to the central Arctic aerosol concentration, *Atmos. Chem. Phys.*, 11, 3093–3105, doi:10.5194/acp-11-3093-2011, 2011a.
- Held, A., Orsini, D. A., Vaattovaara, P., Tjernström, M., and Leck, C.: Near-surface profiles of aerosol number concentration and temperature over the Arctic Ocean, *Atmos. Meas. Tech.*, 4, 1603–1616, doi:10.5194/amt-4-1603-2011, 2011b.
- Intrieri, J. M., Shupe, M. D., Uttal, T., and McCarty, B. J.: An annual cycle of Arctic cloud characteristics observed by radar and lidar at SHEBA, *J. Geophys. Res.*, 107, 8030, doi:10.1029/2000JC000423, 2002.
- IUPAC, Analytical Chemistry Division. Nomenclature, symbol, units and their usage in spectrochemical analysis. II. Data interpretation, *Spectrochim. Acta B*, 33, 241–246, 1978.
- Karl, M., Leck, C., Coz, E., and Heintzenberg, J.: Marine nanogels as a source of atmospheric nanoparticles in the high Arctic, *Geophys. Res. Lett.*, 40, 3738–3743, doi:10.1002/grl.50661, 2013.
- Kuznetsova, M., Lee, C., and Aller, J.: Characterization of the proteinaceous matter in marine aerosols, *Mar. Chem.*, 96, 359–377, 2005.
- Leck, C. and Bigg, E. K.: Aerosol production over remote marine areas – A new route, *Geophys. Res. Lett.*, 23, 3577–3581, 1999.
- Leck, C. and Bigg, E. K.: Evolution of the marine aerosol – A new perspective, *Geophys. Res. Lett.*, 32, L19803, doi:10.1029/2005GL023651, 2005a.
- Leck, C. and Bigg, E. K.: Biogenic particles in the surface microlayer and overlying atmosphere in the central Arctic Ocean during summer, *Tellus B*, 57, 305–316, 2005b.
- Leck, C. and Bigg, E. K.: Comparison of sources and nature of the tropical aerosol with the summer high Arctic aerosol, *Tellus B*, 60, 118–126, doi:10.1111/j.1600-0889.2007.00315.x, 2008.
- Leck, C. and Bigg, E. K.: New particle formation of marine biological origin, *Aerosol Sci. Tech.*, 44, 570–577, 2010.
- Leck, C. and Persson, C.: Seasonal and short-term variability in dimethyl sulfide, sulfur dioxide and biogenic sulfur and sea salt aerosol particles in the arctic marine boundary layer, during summer and autumn, *Tellus B*, 48, 272–299, 1996a.
- Leck, C. and Persson, C.: The central Arctic Ocean as a source of dimethyl sulfide: Seasonal variability in relation to biological activity, *Tellus B*, 48, 156–177, 1996b.
- Leck, C., Bigg, E. K., Covert, D. S., Heintzenberg, J., Maenhaut, W., Nilsson, E. D., and Wiedensohler, A.: Overview of the atmospheric research program during the International Arctic Ocean Expedition of 1991 (IAOE-91) and its scientific results, *Tellus B*, 48, 136–155, 1996.
- Leck, C., Nilsson, E. D., Bigg, E. K., and Bäcklin, L.: Atmospheric program on the Arctic Ocean Expedition 1996 (AOE-96): an overview of scientific goals, experimental approaches, and instruments, *J. Geophys. Res.*, 106, 32051–32067, 2001.
- Leck, C., Norman, M., Bigg, E. K., and Hillamo, R.: Chemical composition and sources of the high Arctic aerosol relevant for cloud formation, *J. Geophys. Res.*, 107, 4135, doi:10.1029/2001JD001463, 2002.
- Leck, C., Tjernström, M., Matrai, P., Swietlicki, E., and Bigg, E. K.: Can marine micro-organisms influence melting of the Arctic pack ice?, *EOS T. Am. Geophys. Un.*, 85, 25–36, 2004.
- Liu, B. Y. H. and Lee, K. W.: Efficiency of membrane and Nucleopore filters for sub-micrometer aerosols, *Environ. Sci. Technol.*, 10, 345–350, 1976.
- Mauritsen, T., Sedlar, J., Tjernström, M., Leck, C., Martin, M., Shupe, M., Sjogren, S., Sierau, B., Persson, P. O. G., Brooks, I. M., and Swietlicki, E.: An Arctic CCN-limited cloud-aerosol regime, *Atmos. Chem. Phys.*, 11, 165–173, doi:10.5194/acp-11-165-2011, 2011.
- Mopper, K., Zhou, J., Sri Ramana, K., Passow, U., Dam, H. G., and Drapeau, D. T.: The role of surface-active carbohydrates in the flocculation of a diatom bloom in a mesocosm, *Deep-Sea Res. Pt. II*, 42, 47–73, 1995.
- Nilsson, E. D.: Planetary boundary layer structure and air mass transport during the International Arctic Ocean Expedition 1991, *Tellus B*, 48, 178–196, 1996.
- Nilsson, E. D. and Bigg, E. K.: Influences on formation and dissipation of high arctic fogs during summer and autumn and their interaction with aerosol, *Tellus B*, 48, 234–253, 1996.
- Nilsson, E. D. and Leck, C.: A pseudo-Lagrangian study of the sulfur budget in the remote Arctic marine boundary layer, *Tellus B*, 54, 213–230, 2002.
- Nilsson, E. D., Rannik, Ü., Swietlicki, E., Leck, C., Aalto, P. P., Norman, M., and Zhou, J.: Turbulent aerosol number fluxes during the Arctic Ocean Expedition 1996, part II: a wind driven source of

- sub micrometers aerosol particles from the sea, *J. Geophys. Res.*, 106, 32139–32154, 2001.
- Norris, S. J., Brooks, I. M., de Leeuw, G., Sirevaag, A., Leck, C., Brooks, B. J., Birch, C. E., and Tjernström, M.: Measurements of bubble size spectra within leads in the Arctic summer pack ice, *Ocean Sci.*, 7, 129–139, doi:10.5194/os-7-129-2011, 2011.
- O'Dowd, C. D., Lowe, J. A., Smith, M. H., and Kaye, A. D.: The relative importance of non-sea-salt sulphate and sea-salt aerosol to the marine cloud condensation nuclei population: An improved multi-component aerosol-cloud droplet parameterization, *Q. J. Roy. Meteor. Soc.*, 125, 1295–1313, 1999.
- Ogren, J. A. and Heintzenberg, J.: Parametric aerosol sampling at low concentration levels: Rap. AA-1, Department of Meteorology, Stockholm University, AA-1, 1990.
- Orellana, M. V. and Verdugo, P.: Ultraviolet radiation blocks the organic carbon exchange between the dissolved phase and the gel phase in the ocean, *Limnol. Oceanogr.*, 48, 1618–1623, 2003.
- Orellana, M. V., Matrai, P. A., Leck, C., Rauschenberg, C. D., Lee, A. M., and Coz, E.: Marine microgels as a source of cloud condensation nuclei in the high Arctic, *P. Natl. Acad. Sci.*, 108, 13612–13617, 2011.
- Ovadnevaite, J., Ceburnis, D., Martucci, G., Bialek, J., Monahan, C., Rinaldi, M., Facchini, M. C., Berresheim, H., Worsnop, D. R., and O'Dowd, C.: Primary marine organic aerosol: A dichotomy of low hygroscopicity and high CCN activity, *Geophys. Res. Lett.*, 38, L21806, doi:10.1029/2011GL048869, 2011.
- Paatero, J., Vaattovaara, P., Vestenius, M., Meinander, O., Makkonen, U., Kivi, R., Hyvärinen, A., Asmi, E., Tjernström, M., and Leck, C.: Finnish contribution to the Arctic Summer Cloud Ocean Study (ASCOS) expedition, Arctic Ocean 2008, *Geophysica*, 45, 119–146, 2009.
- Panagiotopoulos, C. and Sempere, R.: The molecular distribution of combined aldoses in sinking particles in various oceanic conditions, *Mar. Chem.*, 95, 31–49, 2005.
- Posfai, M., Simonics, R., Li, J., Hobbs, P. V., and Buseck, P. R.: Individual aerosol particles from biomass burning in southern Africa: 1. Compositions and size distributions of carbonaceous particles, *J. Geophys. Res.*, 108, 8483, doi:10.1029/2002JD002291, 2003.
- Rolph, G. D.: Real-time Environmental Applications and Display sYstem (READY) Website (<http://ready.arl.noaa.gov>), NOAA Air Resources Laboratory, Silver Spring, MD., 2011.
- Russell, L. M., Hawkins, L. N., Frossard, A. A., Quinn, P. K., and Bates, T. S.: Carbohydrate like composition of submicron atmospheric particles and their production from ocean bubble bursting, *P. Natl. Acad. Sci. USA*, 107, 6652–6657, doi:10.1073/pnas.0908905107, 2010.
- Sedlar, J., Tjernström, M., Mauritsen, T., Shupe, M. D., Brooks, I. M., Persson, P. O. G., Birch, C. E., Leck, C., Sirevaag, A., and Nicolaus, M.: A transitioning Arctic surface energy budget: the impacts of solar zenith angle, surface albedo and cloud radiative forcing, *Clim. Dynam.*, 37, 1643–1660, doi:10.1007/s00382-010-0937-5, 2011.
- Shupe, M. D., Persson, P. O. G., Brooks, I. M., Tjernström, M., Sedlar, J., Mauritsen, T., Sjogren, S., and Leck, C.: Cloud and boundary layer interactions over the Arctic sea ice in late summer, *Atmos. Chem. Phys.*, 13, 9379–9399, doi:10.5194/acp-13-9379-2013, 2013.
- Skoog, A. and Benner, R.: Aldoses in various size fractions of marine organic matter: Implications for carbon cycling, *Limnol. Oceanogr.*, 42, 1803–1813, 1998.
- Tjernström, M.: The summer Arctic boundary layer during the Arctic Ocean Experiment 2001 (AOE-2001), *Bound.-Lay. Meteorol.*, 117, 5–36, 2005.
- Tjernström, M., Birch, C. E., Brooks, I. M., Shupe, M. D., Persson, P. O. G., Sedlar, J., Mauritsen, T., Leck, C., Paatero, J., Szczodrak, M., and Wheeler, C. R.: Meteorological conditions in the central Arctic summer during the Arctic Summer Cloud Ocean Study (ASCOS), *Atmos. Chem. Phys.*, 12, 6863–6889, doi:10.5194/acp-12-6863-2012, 2012.
- Tjernström, M., Leck, C., Birch, C. E., Brooks, B. J., Brooks, I. M., Bäcklin, L., Chang, R. Y.-W., Granath, E., Graus, M., Hansel, A., Heintzenberg, J., Held, A., Hind, A., de la Rosa, S., Johnston, P., Knulst, J., de Leeuw, G., Di Liberto, L., Martin, M., Matrai, P. A., Mauritsen, T., Müller, M., Norris, S. J., Orellana, M. V., Orsini, D. A., Paatero, J., Persson, P. O. G., Gao, Q., Rauschenberg, C., Ristovski, Z., Sedlar, J., Shupe, M. D., Sierau, B., Sirevaag, A., Sjogren, S., Stetzer, O., Swietlicki, E., Szczodrak, M., Vaattovaara, P., Wahlberg, N., Westberg, M., and Wheeler, C. R.: The Arctic Summer Cloud-Ocean Study (ASCOS): overview and experimental design, *Atmos. Chem. Phys. Discuss.*, 13, 13541–13652, doi:10.5194/acpd-13-13541-2013, 2013.
- Tominaga, S., Matsumoto, K., Kaneyasu, N., Shigihara, A., Katono, K., and Igawa, M.: Measurements of particulate sugars at urban and forested suburban sites, *Atmos. Environ.*, 45, 2335–2339, 2011.
- Verdugo, P.: Marine Microgels, *Ann. Rev. Mar. Sci.*, 4, 375–400, 2012.
- von der Weiden, S.-L., Drewnick, F., and Borrmann, S.: Particle Loss Calculator – a new software tool for the assessment of the performance of aerosol inlet systems, *Atmos. Meas. Tech.*, 2, 479–494, doi:10.5194/amt-2-479-2009, 2009.
- Xin, L., Leck, C., Sun, L., Hede, T., Tu, Y., and Ågren, H.: Cross-Linked Polysaccharide Assemblies in Marine Gels: An Atomistic Simulation, *J. Phys. Chem. Lett.*, 4, 2637–2642, doi:10.1021/jz401276r, 2013.
- Zhou, J., Mopper, K., and Passow, U.: The role of surface-active carbohydrates in the formation of transparent exopolymer particles by bubble adsorption of seawater, *Limnol. Oceanogr.*, 43, 1860–1871, 1998.